# Design of Low-Density Parity-Check Codes for Modulation and Detection

Stephan ten Brink, Gerhard Kramer, *Member, IEEE*, and Alexei Ashikhmin, *Member, IEEE*

***Abstract*—A coding and modulation technique is studied where the coded bits of an irregular low-density parity-check (LDPC) code are passed directly to a modulator. At the receiver, the variable nodes of the LDPC decoder graph are connected to detector nodes, and iterative decoding is accomplished by viewing the variable and detector nodes as one decoder. The code is optimized by performing a curve fitting on extrinsic information transfer charts. Design examples are given for additive white Gaussian noise channels, as well as multiple-input, multiple-output (MIMO) fading channels where the receiver, but not the transmitter, knows the channel. For the MIMO channels, the technique operates within 1.25 dB of capacity for various antenna configurations, and thereby outperforms a scheme employing a parallel concatenated (turbo) code by wide margins when there are more transmit than receive antennas.**

***Index Terms*—Fading, iterative decoding, low-density parity-check (LDPC) codes, multiple-input, multiple-output (MIMO) detection, mutual information.**

## I. Introduction

ITERATIVE decoding of low-density parity-check (LDPC) codes is a powerful method for approaching capacity on noisy channels [1]–[5]. We consider two problems associated with LDPC codes. The first is how to combine a code with a modulator and detector. The second is how to design the code for iterative decoding, i.e., how to choose good degree distributions for the modulator, channel, and detector.

We approach the first problem by mapping the coded bits of an irregular LDPC code directly onto a modulation signal set. The mapping is arranged to facilitate code design. At the receiver, we consider the graphical representation of an LDPC decoder [2]–[4] and connect the LDPC variable nodes to detector nodes.

We deal with the second problem by using a *curve-fitting* procedure on extrinsic information transfer (EXIT) charts [6]. The design methodology is illustrated for two types of channels: additive white Gaussian noise (AWGN) channels with binary phase-shift keying (BPSK), and multiple-input, multiple-output (MIMO) fading channels with quadrature phase-shift keying (QPSK). The MIMO code design can be be extended in a straightforward way to other modulators, channels, and detectors. We remark that the curve fitting might be possible using other chart techniques, see, e.g., [5], [7], and [8]. We refer to [9] for a comparison of some of these tools. Another alternative is to use numerical optimization with *density evolution* [3, 4]. Transfer charts and density evolution complement each other in that the former are easier to visualize and program, giving insight and good initial code designs, while the latter can be used to verify the graphical analysis and to refine the designs.

There are several existing approaches to combining coding and modulation, for example, trellis-coded modulation (TCM) [10], multilevel coding [11], bit-interleaved coded modulation (BICM) [12], and space–time block-coded (STBC) modulation [13], [14] (see also [15] and references therein). A growing body of work uses BICM with turbo and LDPC codes, see, e.g., [16]–[29]. The EXIT curve-fitting approach described here was motivated by results for erasure channels [30] and appeared in [31]. Parallel work using similar ideas was reported in [32] and [33]. The method was used to design repeat-accumulate (RA) codes in [34] and [35].

This paper is organized as follows. In Section II, we develop the curve-fitting procedure for BPSK on the AWGN channel. In Section III, we extend the technique to other communication problems, and, in particular, to MIMO fading channels where the receiver, but not the transmitter, knows the channel. We design LDPC codes for ergodic fading, and compare their performance with a scheme employing a universal mobile telecommunications system (UMTS) standard turbo code. The LDPC codes are shown to perform substantially better for channels having more transmit than receive antennas. Such a situation is likely to occur on the base-to-mobile station link of a wireless communication system. Section IV summarizes our results.

## II. Code Design for AWGN Channels

Consider an LDPC code of length $n$ and design rate $R = k/n$. An iterative decoder for this code can be viewed as a graph that has $n$ variable nodes, an edge interleaver, and $n-k$ check nodes. The $i$th variable node represents the $i$th bit of the codeword. This bit is involved in $d_v^{(i)}$ parity checks, so that its node has $d_v^{(i)}$ edges going into the edge interleaver. The edge interleaver connects the variable nodes to the check nodes, each of which represents a parity-check equation. The $i$th check node checks $d_c^{(i)}$ bits so that it has $d_c^{(i)}$ edges. The sets of variable and check nodes are referred to as the variable-node decoder (VND) and check-node decoder (CND), respectively. Iterative decoding is performed by passing messages between the VND and CND.

The decoder structure is shown in Fig. 1, and its operation is explained in more detail below. We remark that this structure is similar to that of an iterative decoder for a serially concatenated

Paper approved by H. El Gamal, the Editor for Space–Time Coding and Spread Spectrum of the IEEE Communications Society. Manuscript received July 17, 2002; revised May 30, 2003.

S. ten Brink was with Bell Laboratories, Lucent Technologies, Crawford, NJ. He is now with Realtek, Irvine, CA 92618 USA (e-mail: stenbrink@realtek-us.com).

G. Kramer and A. Ashikhmin are with Bell Laboratories, Lucent Technologies, Murray Hill, NJ 07974 USA (e-mail: gkr@bell-labs.com; aea@bell-labs.com).

Digital Object Identifier 10.1109/TCOMM.2004.826370

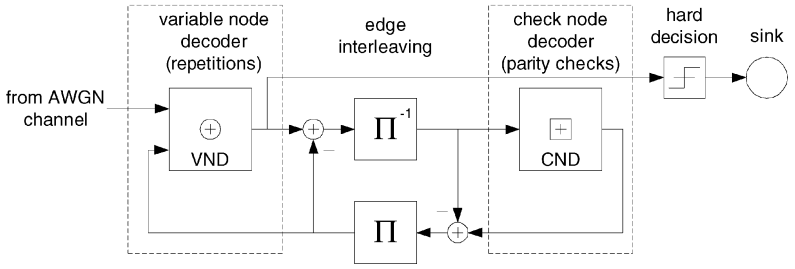


Fig. 1. Iterative decoder for an LDPC code.

code that is based on a mixture of inner repetition codes and a mixture of outer single parity-check codes. This observation illustrates the close relation between LDPC decoding and other iterative schemes, such as turbo decoding [36].

### A. EXIT Charts

An *a posteriori* probability (APP) decoder converts channel and *a priori* log-likelihood ratios (LLRs or L-values) into *a posteriori* L-values. This is shown in Fig. 1, where *a posteriori* L-values come out of the VND and CND. The *a posteriori* L-values minus the *a priori* L-values are the *extrinsic* L-values, which are passed on and interpreted as *a priori* information by a second decoder. We refer to [37] for further details on extrinsic information processing.

An EXIT chart characterizes the decoder's operation. We use the notation of [6] and write $I_A$ for the average mutual information between the bits on the decoder graph edges (which are the bits about which extrinsic L-values are passed) and the *a priori* L-values. Similarly, we write $I_E$ for the average mutual information between the bits on the graph edges and the extrinsic L-values. We refer to [6] for further details on how to interpret these quantities.

### B. EXIT Curve of the Inner VND

A variable node of degree $d_v$ has $d_v + 1$ incoming messages, $d_v$ from the edge interleaver and one from the channel. The variable node decodes by computing, for $i = 1, 2, \ldots, d_v$

$$L_{i,\text{out}} = L_{\text{ch}} + \sum_{j \neq i} L_{j,\text{in}} \tag{1}$$

where $L_{j,\text{in}}$ is the $j$th *a priori* L-value going into the variable node, $L_{i,\text{out}}$ is the $i$th extrinsic L-value coming out of the variable node, and $L_{\text{ch}}$ is the channel L-value.

Consider the AWGN channel with BPSK ($\pm 1$) modulation and noise variance $\sigma_n^2$. We define the normalized signal-to-noise ratio (SNR) as $E_b/N_0 = 1/(2R\sigma_n^2)$. The channel L-value is

$$L_{\text{ch}} := \log \frac{p(y|x=+1)}{p(y|x=-1)} = \frac{2}{\sigma_n^2}\, y \tag{2}$$

where $p(y|x)$ is the channel conditional probability density function (pdf) evaluated at the output $y$ given the input $x$. Let $X$ and $Y$ be random variables representing the respective channel input and output. The variance of $L_{\text{ch}}$ conditioned on $X$ is

$$\sigma_{\text{ch}}^2 = \frac{4}{\sigma_n^2} = 8R \cdot \frac{E_b}{N_0}. \tag{3}$$

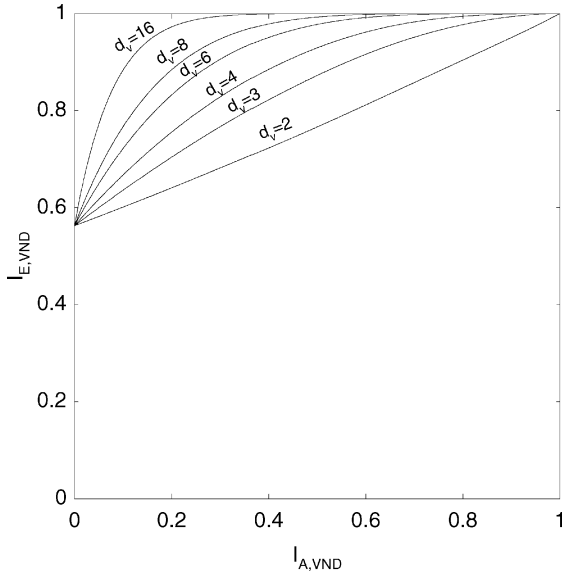


Fig. 2. VND EXIT curves for $E_b/N_0 = 1$ dB and $R = 1/2$.

To compute an EXIT function, we model $L_{j,\text{in}}$ as the output L-value of an AWGN channel whose input is the $j$th interleaver bit transmitted using BPSK. The EXIT function of a degree-$d_v$ variable node is then

$$I_{E,\text{VND}}\left(I_A, d_v, \frac{E_b}{N_0}, R\right) = J\left(\sqrt{(d_v - 1)\left[J^{-1}(I_A)\right]^2 + \sigma_{\text{ch}}^2}\right) \tag{4}$$

where the functions $J(\cdot)$ and $J^{-1}(\cdot)$ are given in the Appendix (see also [6]). Fig. 2 plots several variable node curves when $R = 1/2$ and $E_b/N_0 = 1$ dB. The quantity

$$I_{E,\text{VND}}\left(0, d_v, \frac{E_b}{N_0}, R\right) = J(\sigma_{\text{ch}}) \tag{5}$$

is the capacity of the channel at the $\sigma_{\text{ch}}$ that is being considered, which in our case is the capacity of the AWGN channel with BPSK modulation (see the Appendix).

### C. EXIT Curve of the Outer CND

The decoding of a degree $d_c$ check node corresponds to the decoding of a length $d_c$ (or rate $(d_c - 1)/d_c$) single parity-check code. The output L-values are thus (see [37, Sec. II.A])

$$L_{i,\text{out}} = \ln \frac{1 - \prod_{j \neq i} \dfrac{1 - e^{L_{j,\text{in}}}}{1 + e^{L_{j,\text{in}}}}}{1 + \prod_{j \neq i} \dfrac{1 - e^{L_{j,\text{in}}}}{1 + e^{L_{j,\text{in}}}}}. \tag{6}$$

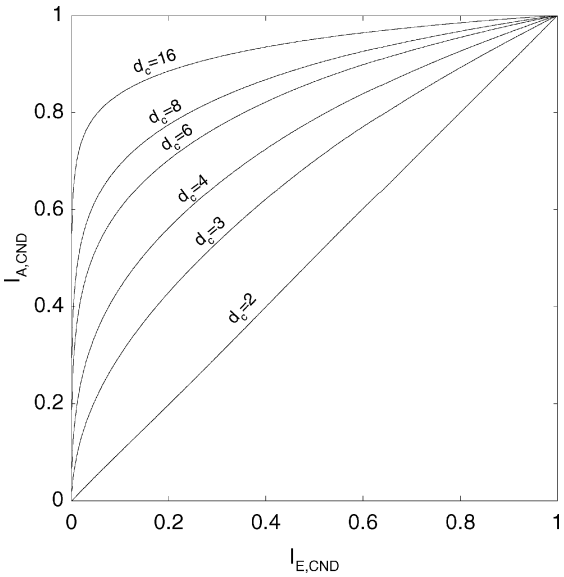


Fig. 3. CND EXIT curves. Observe that the *a priori* and extrinsic axes are swapped, as compared with Fig. 2.

In the L-value notation of [37], this can also be written as a "box-plus" operation

$$L_{i,\text{out}} = \sum_{j \neq i} \boxplus L_{j,\text{in}}. \tag{7}$$

We again model $L_{j,\text{in}}$ as the output L-value of an AWGN channel whose input is the $j$th interleaver bit transmitted using BPSK. The check node EXIT curves can be computed in closed form [38], [46] or by simulation. Alternatively, for the binary erasure channel, a duality property exists [5], [30] that gives the EXIT curve $I_{E,\text{SPC}}(\cdot)$ of the length $d_c$ single parity-check code in terms of the EXIT curve $I_{E,\text{REP}}(\cdot)$ of the length $d_c$ (or rate $1/d_c$) repetition code, i.e.,

$$I_{E,\text{SPC}}(I_A, d_c) = 1 - I_{E,\text{REP}}\left(1 - I_A, d_c\right). \tag{8}$$

This property is not exact for BPSK/AWGN *a priori* inputs, but it is very accurate [38], [46]. For convenience, we use (8) and write

$$\begin{aligned} I_{E,\text{CND}}(I_A, d_c) &\approx 1 - I_{E,\text{REP}}\left(1 - I_A, d_c\right) \\ &= 1 - J\left(\sqrt{d_c - 1} \cdot J^{-1}\left(1 - I_A\right)\right) \end{aligned} \tag{9}$$

where the second step follows from (4) with $\sigma_{\text{ch}}^2 = 0$. It is further useful to express (9) in terms of its inverse function, i.e.,

$$I_{A,\text{CND}}(I_E, d_c) \approx 1 - J\left(\frac{J^{-1}\left(1 - I_E\right)}{\sqrt{d_c - 1}}\right). \tag{10}$$

Fig. 3 plots several check node curves. Observe that the curves are similar to the VND curves of Fig. 2, except that they all start from the origin.

### D. EXIT Curves for Code Mixtures

We will consider only *check-regular* LDPC codes, i.e., all check nodes have degree $d_c$ (in [39], these are called *right-regular* codes). After choosing $d_c$, the remaining LDPC design involves specifying the variable node degrees $d_v^{(i)}$, $i = 1, \ldots, n$. Let $D$ be the number of different variable node degrees, and denote these degrees by $d_{v,i}$, $i = 1, \ldots, D$. The average variable node degree is

$$\overline{d}_v = \sum_{i=1}^{D} a_i \cdot d_{v,i} \tag{11}$$

where $a_i$ is the fraction of *nodes* having degree $d_{v,i}$. Note that the $a_i$ must satisfy $\sum_i a_i = 1$. Since the number of edges at the VND and CND are the same, we have $n\,\overline{d}_v = (n - k)\,d_c$ or

$$\overline{d}_v = (1 - R) \cdot d_c. \tag{12}$$

Let $b_i$ be the fraction of *edges* incident to variable nodes of degree $d_{v,i}$. There are, in total, $(n\,a_i)\,d_{v,i}$ edges involved with such nodes, so we have

$$b_i = \frac{n\,a_i\,d_{v,i}}{n\,\overline{d}_v} = \frac{d_{v,i}}{(1 - R)\,d_c} \cdot a_i. \tag{13}$$

Note that the $b_i$ must satisfy $\sum_i b_i = 1$. In [30] and [40], it is shown that the EXIT curve of a mixture of codes is an average of the component EXIT curves. We must here average using the $b_i$ (and not the $a_i$) because it is the *edges* that carry the extrinsic messages. The effective VND transfer curve is thus

$$I_{E,\text{VND}}\left(I_A, \frac{E_b}{N_0}, R\right) = \sum_{i=1}^{D} b_i \cdot I_{E,\text{VND}}\left(I_A, d_{v,i}, \frac{E_b}{N_0}, R\right) \tag{14}$$

i.e., (14) is a weighted sum of the curves of Fig. 2. Note that only $D - 2$ edge fractions can be adjusted because we must enforce (12) and $\sum_i b_i = 1$. Thus, in order to have any flexibility, we must choose $D \geq 3$. We shall see that $D = 3$ already gives surprisingly good results [4, p. 634].

### E. Design Example

The paper [30] (see also [40]) shows that to approach capacity on erasure channels, one must match the VND and CND transfer curves. Empirically, the same is true for other channels. We illustrate this for BPSK modulation on an AWGN channel, and in the next section for MIMO channels.

Recall that $I_{E,\text{VND}}(0, E_b/N_0, R)$ is the channel capacity (see the Appendix). We design a code with $R = 1/2$, and choose $E_b/N_0 = 0.5$ dB, so that $I_{E,\text{VND}}(0, 0.5\text{ dB}, 1/2) \approx 0.524$ is slightly larger than $R$. We further choose $d_c = 8$ so that the CND transfer curve has a reasonable distance from the $y$ axis at $I_{A,\text{CND}} = 1/2$. This approach simplifies finding a VND curve that lies above the CND curve. Furthermore, this gives the decoder a good "head start" at the first iteration.

For simplicity, we restrict the VND to have only three different variable node degrees ($D = 3$). This means that only one $b_i$ can be chosen freely, and Fig. 4 shows a manual curve fit whose variable node parameters are as follows:

$$\begin{aligned} d_{v,1} &= 2, \quad a_1 = 0.508, \quad b_1 = 0.254 \\ d_{v,2} &= 4, \quad a_2 = 0.419, \quad b_2 = 0.419 \\ d_{v,3} &= 18, \quad a_3 = 0.073, \quad b_3 = 0.327. \end{aligned}$$

For this simple example, we obtain a convergence threshold of about 0.5 dB, while the capacity is at 0.19 dB. A simulation with $n = 10^5$, a random edge interleaver, and 100 iterations shows a turbo cliff at about 0.55 dB (we measure the turbo cliff

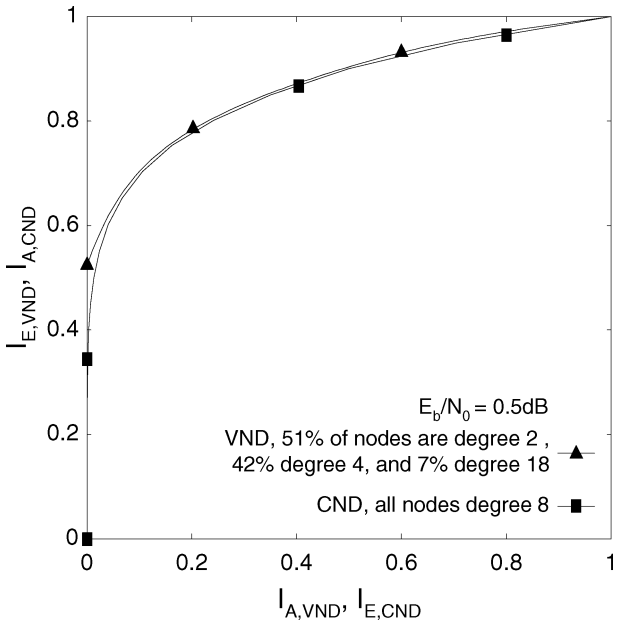


Fig. 4. Curve fit for an LDPC code with $R = 1/2$.

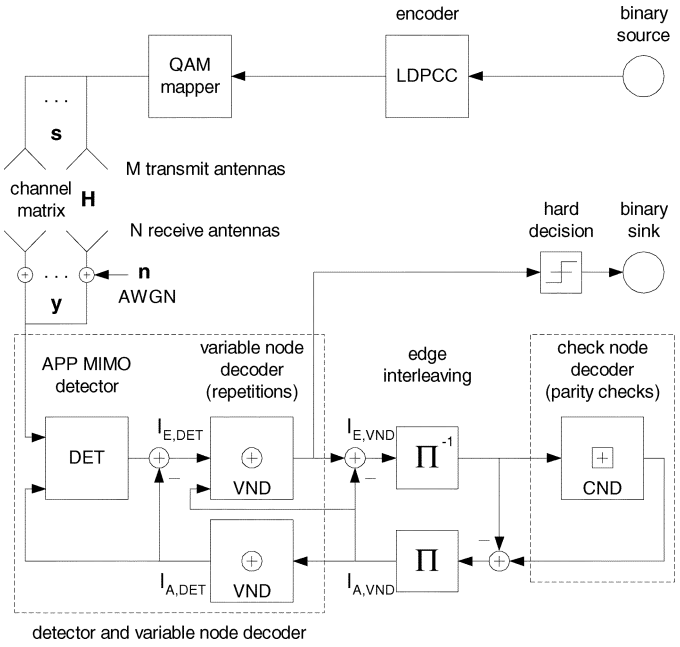


Fig. 5. MIMO model.

at a bit-error rate (BER) of $10^{-4}$). For longer codes and more iterations, the turbo cliff is at 0.5 dB, which verifies the accuracy of the EXIT chart and our approximations.

We remark that by choosing larger $D$, one can match the VND curve more closely to the CND curve. One can also model the *a priori* L-values more carefully than as outputs of an AWGN channel. Finally, code design is just as easy for other rates. For instance, suppose that $R = 3/4$ so that the VND curve should start at about $(I_{A,\mathrm{VND}}, I_{E,\mathrm{VND}}) = (0, 3/4)$. Fig. 3 suggests that $d_c = 16$ can yield a good curve fit. We would now again choose the $b_i$ to ensure that the $I_{E,\mathrm{VND}}(\cdot)$ curve lies above the $I_{A,\mathrm{CND}}(\cdot) = I^{-1}_{E,\mathrm{CND}}(\cdot)$ curve.

## III. Code Design for MIMO Channels

We next turn to multiantenna modulation and detection. The techniques described here can be applied to many other modulators, channels, and detectors.

### A. MIMO Channel Model

For MIMO fading, one often distinguishes between three practical cases based on channel knowledge. The first case is that both the transmitter and receiver know the channel, the second that only the receiver knows the channel, and the third that neither terminal knows the channel [41, pp. 2627–2629]. The first case can be dealt with in a manner similar to the AWGN channel, with the addition of "water pouring" over the antennas and time. The third case seems to be the most difficult and is not dealt with here. We will consider only the second case.

Consider the setup of Fig. 5, where there are $M$ transmit and $N$ receive antennas. Each transmitter symbol is an $M \times 1$ vector $\mathbf{s} = [s_1, \ldots, s_M]^T$ whose entries take on complex values in a constellation set. We consider constellations of size $2^{M_c}$ so that each vector symbol carries $M \cdot M_c$ coded bits. For example, for QPSK, we have $M_c = 2$. The average energy per transmit symbol is limited to $E_s$, and we will use $E[\|s_m\|^2] = E_s/M$ for $m = 1, 2, \ldots, M$.

The receiver sees $N \times 1$ vectors $\mathbf{y} = \mathbf{H}\mathbf{s} + \mathbf{n}$, where $\mathbf{H}$ is the $N \times M$ channel matrix and $\mathbf{n}$ is a $N \times 1$ noise vector. Suppose the entries of $\mathbf{n}$ are independent, complex, zero-mean, Gaussian random variables with independent real and imaginary parts each having variance $\sigma_n^2 = N_0/2$. We define the normalized SNR $E_b/N_0$ as

$$\left.\frac{E_b}{N_0}\right|_{\mathrm{dB}} = \left.\frac{E_s}{N_0}\right|_{\mathrm{dB}} + 10\log_{10}\frac{N}{RMM_c}. \tag{15}$$

The value $N$ appears in (15) by convention; this is done simply to keep the $E_b/N_0|_{\mathrm{dB}}$ at capacity close to each other for different $N$. We assume that $\mathbf{H}$ is known to the receiver only, and consider a Rayleigh fading channel, so that the entries of $\mathbf{H}$ are independent, complex, zero-mean, Gaussian random variables with independent real and imaginary parts each having variance 1/2 [42, Sec. 4]. For a *quasi-static* channel, the matrix $\mathbf{H}$ remains unchanged over long time intervals, while for an *ergodic* channel, $\mathbf{H}$ changes for every symbol $\mathbf{s}$. We consider only the ergodic model whose capacity is (see [42] and [43])

$$C = E\left[\log_2 \det\left(\mathbf{I} + \frac{E_s}{N_0}\frac{1}{M}\mathbf{H}\mathbf{H}^{\dagger}\right)\right] \tag{16}$$

where $\mathbf{I}$ is the identity matrix and $\mathbf{H}^{\dagger}$ is the complex-conjugate transpose of $\mathbf{H}$. One achieves capacity with Gaussian distributed $\mathbf{s}$. We will consider only QPSK for simplicity, but the design procedure described below is the same for other modulation sets and mappings (see [34]).

### B. EXIT Curve of the MIMO Detector

We proceed by showing how to compute EXIT curves for the MIMO detector. We then describe a combined demodulation/decoding structure that is flexible enough to closely approach MIMO capacity. This structure automatically specifies

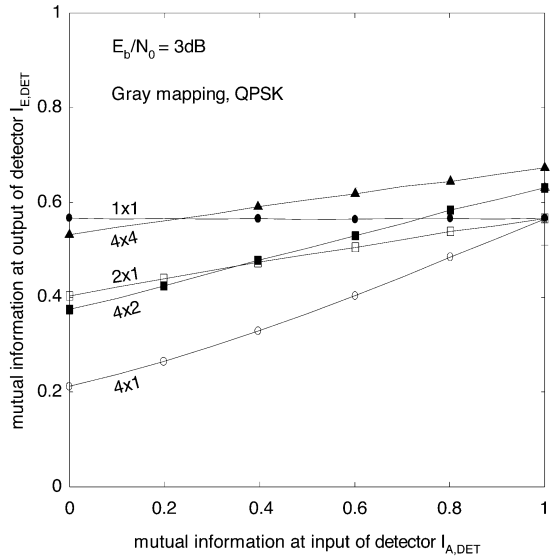


Fig. 6. MIMO detector EXIT curves at $E_b/N_0 = 3$ dB and $R = 1/2$.

how the encoding/modulation is done, i.e., one maps the coded bits directly onto the modulation signal set. Finally, we show how to match EXIT curves.

The MIMO detector performs APP detection by considering all $2^{MM_c}$ possible hypotheses on $\mathbf{s}$ (see [16]–[20]). That is, the detector computes the L-values

$$\log \frac{\Pr(c_i = 0|\mathbf{y})}{\Pr(c_i = 1|\mathbf{y})} \tag{17}$$

for $i = 1, 2, \ldots, MM_c$, where $c_i$ is the $i$th coded bit mapped onto the vector symbol $\mathbf{s}$ whose channel output is $\mathbf{y}$. The detector EXIT curve cannot be described in closed form, so we measure it by Monte Carlo simulation [20]. We denote the detector by DET and its EXIT curve by

$$I_{E,\mathrm{DET}}\left(I_{A,\mathrm{DET}}, \frac{E_b}{N_0}, R\right). \tag{18}$$

Fig. 6 shows simulated EXIT curves of MIMO detectors for Gray-mapped QPSK, and different numbers of transmit and receive antennas. Observe that most of the curves resemble straight lines. The $1 \times 1$ curve is, in fact, the horizontal line

$$I_{E,\mathrm{DET}}\left(I_{A,\mathrm{DET}}, \frac{E_b}{N_0}, R\right) = E\left[J\left(\sqrt{8R\frac{E_b}{N_0}\cdot|H|^2}\right)\right] \tag{19}$$

where $H$ is a zero-mean, unit-variance, complex Gaussian random variable, and where we have used (5). We remark that any $1 \times N$ curve is a horizontal line. Furthermore, the $M \times 1$ curves meet at $I_{A,\mathrm{DET}} = 1$, and the curves decrease with $M$ when $N = 1$. Similarly, one can show analytically that the $M \times N$ curves meet the $1 \times N$ curve at $I_{A,\mathrm{DET}} = 1$, and that they decrease with $M$ for fixed $I_{A,\mathrm{DET}}$ and $N$.

### C. EXIT Curve of the Combined MIMO Detector and VND

We combine the MIMO detector and the LDPC variable node decoder as shown in Fig. 5. The detector consists of $n/(MM_c)$ individual detectors (or detector nodes) that are each connected to $MM_c$ variable nodes. We further choose all $MM_c$ variable nodes connected to a common detector node to have the same degree $d_v$. This restriction is not necessary, but it simplifies the design by focusing on a smaller set of EXIT curves.

The decoder structure specifies that the LDPC coded bits be mapped directly onto the modulation set. A similar technique has been considered by others, e.g., [26] and [27], but without the structured combination of variable and detector nodes, and without the EXIT curve matching approach to code design. We show that curve matching gives coded modulations that closely approach capacity.

Consider the three boxes in Fig. 5 corresponding to one of the $n/(MM_c)$ individual detector/VNDs. We denote the EXIT curve of this structure by $I_{E,\mathrm{VND}}(\cdot)$. We again model the *a priori* L-values as the output L-values of an AWGN channel whose inputs are the interleaver bits transmitted using BPSK. Using (4), the lower VND in Fig. 5 maps $I_{A,\mathrm{VND}}$ into

$$I_{A,\mathrm{DET}}(I_{A,\mathrm{VND}}, d_v) = J\left(\sqrt{d_v}\cdot J^{-1}\left(I_{A,\mathrm{VND}}\right)\right). \tag{20}$$

We next approximate the detector curve (18) by a third-order polynomial. For example, the EXIT curve of the $4 \times 1$ MIMO detector with QPSK at $E_b/N_0 = 7$ dB and $R = 1/2$ is well approximated as

$$\begin{aligned} &I_{E,\mathrm{DET}}\left(I_{A,\mathrm{DET}}, 7\text{ dB}, \frac{1}{2}\right) \\ &= -0.171\cdot I_{A,\mathrm{DET}}^3 + 0.271\cdot I_{A,\mathrm{DET}}^2 + 0.393\cdot I_{A,\mathrm{DET}} + 0.269. \end{aligned} \tag{21}$$

The polynomial (21) lets us express the combined detector/VND curve in closed form, which is convenient for curve fitting.

The third step is to consider the upper VND in Fig. 5. We use (4) with $\sigma_{\mathrm{ch}}^2 = \left[J^{-1}\left(I_{E,\mathrm{DET}}\right)\right]^2$ and write the combined detector/VND EXIT curve as

$$\begin{aligned} &I_{E,\mathrm{VND}}\left(I_{A,\mathrm{VND}}, I_{E,\mathrm{DET}}, d_v\right) \\ &= J\left(\sqrt{(d_v-1)\left[J^{-1}\left(I_{A,\mathrm{VND}}\right)\right]^2 + \left[J^{-1}\left(I_{E,\mathrm{DET}}\right)\right]^2}\right). \end{aligned} \tag{22}$$

Finally, inserting (18), (20), and the detector polynomial (21) into (22), we obtain the desired transfer curve in the form

$$I_{E,\mathrm{VND}}\left(I_{A,\mathrm{VND}}, d_v, \frac{E_b}{N_0}, R\right). \tag{23}$$

Fig. 7 shows some combined detector and VND transfer curves. Observe that by setting $d_v = 1$ in (23) we recover the "pure" detector transfer curves of Fig. 6.

### D. Design Examples

We design check-regular LDPC codes by matching the curve (23) to a CND curve (9). We again restrict ourselves to just three different variable node degrees ($D = 3$) and perform the curve fit manually. Table I shows the parameters of our curve fitting for several MIMO channels, and Fig. 8 plots the resulting EXIT chart for a $4 \times 1$ MIMO channel.

Fig. 9 and Table I give simulation results for LDPC codes with Gray-mapped QPSK, $R = 1/2$, $n = 10^5$, a random edge interleaver, and 100 decoder iterations. All schemes operate within 1.25 dB of their respective capacity limits (due to the complexity of the APP processing, the number of simulated blocks for the

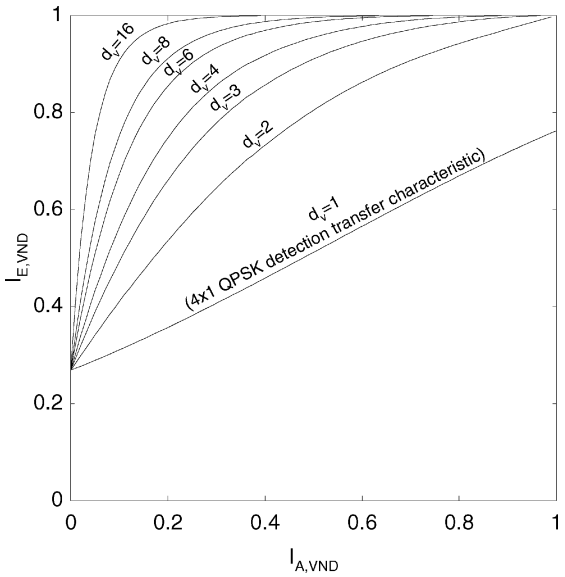


Fig. 7. Combined $4 \times 1$-detector and VND EXIT curves at $E_b/N_0 = 7$ dB and $R = 1/2$.

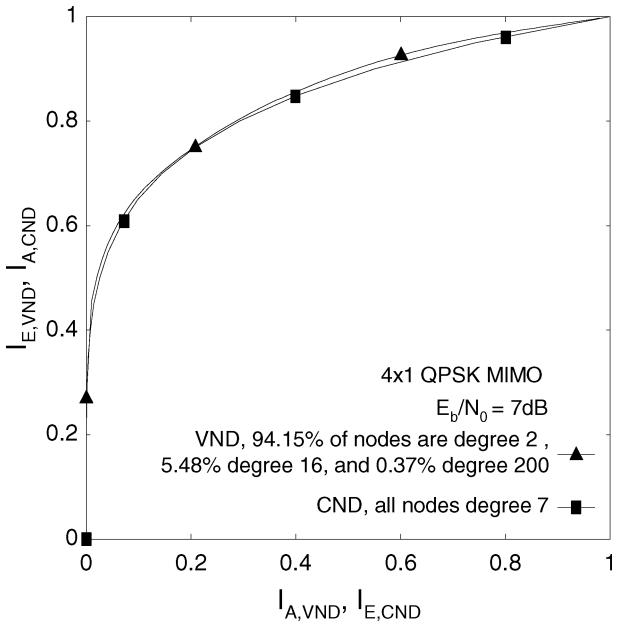


Fig. 8. Curve fit for the $4 \times 1$ scheme at $E_b/N_0 = 7$ dB and $R = 1/2$.

TABLE I
LDPC CODE PARAMETERS FOR $M \times N$ MIMO CHANNELS, QPSK, AND $R = 1/2$. OVERALL RATE: $M$ BITS/CHANNEL USE

| $2 \times 1$ | | |
|---|---|---|
| Capacity $E_b/N_0$ at 3.25dB | | |
| Curve fit at 3.50dB | | |
| BER $10^{-4}$ at 4.00dB (PCC at 5.00dB) | | |
| $d_c = 8$ | | |
| $d_{v,i}$ | $a_i$ [%] | $b_i$ [%] |
| 2 | 48.04 | 24.02 |
| 3 | 45.52 | 34.14 |
| 26 | 6.44 | 41.84 |

| $4 \times 1$ | | | $4 \times 2$ | | |
|---|---|---|---|---|---|
| Capacity $E_b/N_0$ at 6.65dB | | | Capacity $E_b/N_0$ at 2.95dB | | |
| Curve fit at 7.00dB | | | Curve fit at 3.30dB | | |
| BER $10^{-4}$ at 7.90dB (PCC at 13.8dB) | | | BER $10^{-4}$ at 3.60dB (PCC at 5.40dB) | | |
| $d_c = 7$ | | | $d_c = 6$ | | |
| $d_{v,i}$ | $a_i$ [%] | $b_i$ [%] | $d_{v,i}$ | $a_i$ [%] | $b_i$ [%] |
| 2 | 94.15 | 53.80 | 2 | 69.78 | 46.52 |
| 16 | 5.48 | 25.05 | 3 | 26.12 | 26.12 |
| 200 | 0.37 | 21.15 | 20 | 4.10 | 27.36 |

| $4 \times 3$ | | | $4 \times 4$ | | |
|---|---|---|---|---|---|
| Capacity $E_b/N_0$ at 1.97dB | | | Capacity $E_b/N_0$ at 1.47dB | | |
| Curve fit at 2.30dB | | | Curve fit at 1.80dB | | |
| BER $10^{-4}$ at 2.45dB (PCC at 3.20dB) | | | BER $10^{-4}$ at 1.95dB (PCC at 2.40dB) | | |
| $d_c = 7$ | | | $d_c = 8$ | | |
| $d_{v,i}$ | $a_i$ [%] | $b_i$ [%] | $d_{v,i}$ | $a_i$ [%] | $b_i$ [%] |
| 2 | 49.49 | 28.28 | 2 | 33.83 | 16.91 |
| 3 | 43.88 | 37.61 | 3 | 59.80 | 44.85 |
| 18 | 6.63 | 34.11 | 24 | 6.37 | 38.24 |

$4 \times N$ cases was limited to 40). We expect that the gaps to capacity can be narrowed further by using $D > 3$ and better curve fits, and by using longer codes and more iterations.

Fig. 9 also plots the BER curves of BICM employing a UMTS standard turbo code, denoted PCC for "parallel concatenated code." The PCC has memory three constituent codes, with feedback and feedforward generator polynomials $1 + D^2 + D^3$ and $1+D+D^3$, respectively. The modulation is again Gray-mapped QPSK and the code has $R = 1/2$, $n = 10^5$, and a random interleaver. The iterative processing is done by performing 20 internal decoder iterations per detector/decoder iteration, and four detector/decoder iterations. More internal or detector/decoder iterations hardly improve the BER.

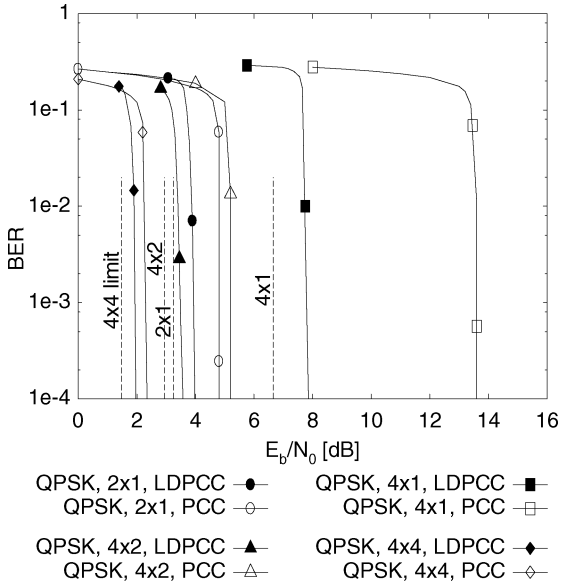


Fig. 9. BERs for LDPC codes (LDPCC) and turbo codes (parallel concatenated codes or PCC). All schemes have an overall rate of $M$ bits per channel use.

Observe that the LDPC scheme outperforms the turbo-coded scheme by wide margins for $M > N$ (the gain is over 5 dB for $4 \times 1$ MIMO). This happens because the turbo code EXIT curve is almost a horizontal line, as will be the case for any strong code, for the AWGN channel. The code EXIT curve is, therefore, poorly matched to a steep detector EXIT curve [20].

### E. Fading Model and Finite Modulation Sets

We discuss two practical issues. First, the ergodic model is suitable if there appear many independent realizations of $\mathbf{H}$, and the receiver can accurately estimate these. This occurs in practice when there is block fading (such as with time-division multiple access, or with multicarrier modulation employing time/frequency interleaving), and one can afford to code over many blocks. However, in some cases, the delay constraints are too severe to code over many blocks, and the quasi-static model is appropriate [42, Sec. 5]. For such cases, one can still apply curve fitting, but one now shapes the EXIT curves to minimize *outage probability*. The question of how to do this precisely for given fading statistics is an interesting open problem.

Second, the capacities of both the ergodic and quasi-static models are achieved with *Gaussian* input distributions. However, in practice, one does not use such distributions. Some reasons for this are the transmitter and receiver amplifiers have peak energy constraints, the amplifiers are linear over limited ranges of inputs, the receiver must acquire and maintain phase synchronization, and the APP detector complexity grows exponentially with the number of bits per input symbol. These reasons make small modulation sets such as QPSK attractive for wireless communication. Of course, the capacities of such modulation sets are smaller than for Gaussian inputs. We have compared the performance of our codes with the finite modulation set capacities, which is the fairest benchmark.

### F. Comparison With STBCs

STBCs are attractive because they improve *diversity* and are easy to encode and decode (see [13]–[15] and references therein). However, the gains come at the expense of spectral efficiency. For example, consider the $2 \times 1$ MIMO channel with QPSK and a rate-1/2 LDPC code. The spectral efficiency is two bits per channel use. Suppose next that we use Alamouti's space–time code [13] as an inner code. This scheme obtains a diversity gain with what is, in effect, a rate-1/2 repetition code. Thus, to achieve two bits per channel use with a rate-1/2 outer code, one must compensate for the inner-code rate loss by changing the constellation from QPSK to 16-quadrature amplitude modulation (QAM). But recall that 16-QAM complicates amplification, synchronization, and detection.

These issues will be even more pronounced for $4 \times 1$ MIMO channels. For example, the scheme proposed here achieves a spectral efficiency of four bits per channel use with QPSK and a rate-1/2 LDPC code. A corresponding STBC [14], which is, in effect, a rate-1/4 repetition code, would have to use 256-QAM to achieve four bits per channel use with a rate-1/2 outer code. Furthermore, no rate-1/4 orthogonal STBC exists for the $4 \times 1$ MIMO channel [14]. These considerations suggest that diversity is best achieved by designing the coding and modulation together rather than separately.

## IV. Summary

We described a method for combining an irregular LDPC code with a modulator and detector. We further introduced a pragmatic technique for designing LDPC degree distributions that are well matched to detectors. The design was based on curve fitting on EXIT charts. For MIMO communication, simulations verified that all our codes operate within 1.25 dB of their respective capacity limits at a BER of $10^{-4}$. We remark that EXIT curve fitting can be used to construct equally good coded modulations with RA codes [34], [35].

Finally, the goal of this paper was to present a coding and modulation technique, as well as a design methodology, that gives good performance for many communication systems. We were less ambitious with our code designs. The LDPC degree distributions listed in Table I can almost certainly be improved upon, especially for the $4 \times 1$ MIMO channel. Other open problems are EXIT curve fitting for quasi-static channels, EXIT curve fitting for suboptimal detectors, e.g., the detectors of several papers in [44], and improving the EXIT approximations.

## Appendix

Consider $Y = X + N$, where $\Pr(X = \pm 1) = 1/2$ and $N$ is zero-mean, Gaussian noise with variance $\sigma_n^2$. The channel L-value of (2) is a function of $y$, and we write this as $L_{\rm ch}(y)$. Note that $L_{\rm ch}(Y)$ conditioned on $X = \pm 1$ is Gaussian with mean $\mu_{\rm ch} = \pm 2/\sigma_n^2$ and variance $\sigma_{\rm ch}^2 = 4/\sigma_n^2$. We thus have

$$\mu_{\rm ch} = \frac{\pm \sigma_{\rm ch}^2}{2}.$$

Let $J(\sigma_{\rm ch})$ be the mutual information $I(X; L_{\rm ch}(Y))$. We have

$$\begin{aligned} J(\sigma_{\rm ch}) &= H(X) - H(X|L_{\rm ch}(Y)) \\ &= 1 - \int_{-\infty}^{\infty} \frac{e^{-\left(\xi - \sigma_{\rm ch}^2/2\right)^2/2\sigma_{\rm ch}^2}}{\sqrt{2\pi\sigma_{\rm ch}^2}} \cdot \log_2\left[1 + e^{-\xi}\right] d\xi \end{aligned} \quad (24)$$

where $H(X)$ is the entropy of $X$ and $H(X|L_{ch}(Y))$ is the entropy of $X$ conditioned on $L_{\rm ch}(Y)$. Note that $I(X; L_{\rm ch}(Y))$ is the same as $I(X;Y)$. The capacity of our $Y = X + N$ channel is, therefore, $J(\sigma_{\rm ch}) = J(2/\sigma_n)$.

For computer implementation, we split $J(\cdot)$ into two parts, corresponding to the intervals $0 \le \sigma \le \sigma^*$ and $\sigma < \sigma^*$ where $\sigma^* = 1.6363$. We used a polynomial fit for the left interval and an exponential fit for the right interval. We applied the Marquardt–Levenberg algorithm (see [45]) to obtain

$$J(\sigma) \approx \begin{cases} a_{J,1}\,\sigma^3 + b_{J,1}\,\sigma^2 + c_{J,1}\,\sigma, & 0 \le \sigma \le \sigma^* \\ 1 - e^{a_{J,2}\,\sigma^3 + b_{J,2}\,\sigma^2 + c_{J,2}\,\sigma + d_{J,2}}, & \sigma^* < \sigma < 10 \\ 1, & \sigma \ge 10 \end{cases}$$

where

$$\begin{aligned} a_{J,1} &= -0.042\,106\,1, \quad b_{J,1} = 0.209\,252 \\ c_{J,1} &= -0.006\,400\,81 \\ a_{J,2} &= 0.001\,814\,91, \quad b_{J,2} = -0.142\,675 \\ c_{J,2} &= -0.082\,205\,4, \quad d_{J,2} = 0.054\,960\,8. \end{aligned}$$

For the inverse $J(\cdot)$-function we split the curve into two intervals at $I^* = 0.3646$. Our approximation is

$$J^{-1}(I) \approx \begin{cases} a_{\sigma,1}\,I^2 + b_{\sigma,1}\,I + c_{\sigma,1}\sqrt{I}, & 0 \le I \le I^* \\ -a_{\sigma,2}\ln\left[b_{\sigma,2}(1-I)\right] - c_{\sigma,2}\,I, & I^* < I < 1 \end{cases}$$

where

$$\begin{aligned} a_{\sigma,1} &= 1.095\,42, \quad b_{\sigma,1} = 0.214\,217, \quad c_{\sigma,1} = 2.337\,27 \\ a_{\sigma,2} &= 0.706\,692, \quad b_{\sigma,2} = 0.386\,013, \quad c_{\sigma,2} = -1.750\,17. \end{aligned}$$

## REFERENCES


[1] R. G. Gallager, "Low-density parity-check codes," *IEEE Trans. Inform. Theory*, vol. IT-8, pp. 21–28, Jan. 1962.

[2] M. G. Luby, M. Mitzenmacher, M. A. Shokrollahi, and D. A. Spielman, "Efficient erasure correcting codes," *IEEE Trans. Inform. Theory*, vol. 47, pp. 569–584, Feb. 2001.

[3] T. J. Richardson and R. L. Urbanke, "The capacity of low-density parity-check codes under message-passing decoding," *IEEE Trans. Inform. Theory*, vol. 47, pp. 599–618, Feb. 2001.

[4] T. J. Richardson, A. Shokrollahi, and R. L. Urbanke, "Design of capacity-approaching low-density parity-check codes," *IEEE Trans. Inform. Theory*, vol. 47, pp. 619–637, Feb. 2001.

[5] S. Y. Chung, G. D. Forney, T. J. Richardson, and R. Urbanke, "On the design of low-density parity-check codes within 0.0045 dB of the Shannon limit," *IEEE Commun. Lett.*, vol. 5, pp. 58–60, Feb. 2001.

[6] S. ten Brink, "Convergence behavior of iteratively decoded parallel concatenated codes," *IEEE Trans. Commun.*, vol. 49, pp. 1727–1737, Oct. 2001.

[7] D. Divsalar, S. Dolinar, and F. Pollara, "Low complexity turbo-like codes," in *Proc. 2nd Int. Symp. Turbo Codes*, Sept. 2000, pp. 73–80.

[8] H. El Gamal and A. R. Hammons, Jr., "Analyzing the turbo decoder using the Gaussian approximation," *IEEE Trans. Inform. Theory*, vol. 47, pp. 671–686, Feb. 2001.

[9] M. Tuechler, S. ten Brink, and J. Hagenauer, "Measures for tracing convergence of iterative decoding algorithms," in *Proc. 4th Int. ITG Conf. Source and Channel Coding*, Berlin, Germany, Jan. 2002, pp. 53–60.

[10] G. Ungerboeck, "Channel coding with multilevel/phase signals," *IEEE Trans. Inform. Theory*, vol. IT-28, pp. 55–67, Jan. 1982.

[11] U. Wachsmann, R. F. H. Fischer, and J. B. Huber, "Multilevel codes: Theoretical concepts and practical design rules," *IEEE Trans. Inform. Theory*, vol. 45, pp. 1361–1391, July 1999.

[12] G. Caire, G. Taricco, and E. Biglieri, "Bit-interleaved coded modulation," *IEEE Trans. Inform. Theory*, vol. 44, pp. 927–946, May 1998.

[13] S. M. Alamouti, "A simple transmit diversity technique for wireless communications," *IEEE J. Select. Areas Commun.*, vol. 16, pp. 1451–1458, Oct. 1998.

[14] V. Tarokh, H. Jafarkani, and A. R. Calderbank, "Space–time block codes from orthogonal designs," *IEEE Trans. Inform. Theory*, vol. 45, pp. 1456–1467, July 1999.

[15] H. El Gamal and M. O. Damen, "Universal space–time coding," *IEEE Trans. Inform. Theory*, vol. 49, pp. 1097–1119, May 2003.

[16] A. M. Tonello, "Space–time bit-interleaved coded modulation with an iterative decoding strategy," in *Proc. Vehicular Technology Conf.*, Sept. 2000, pp. 473–478.

[17] A. van Zelst, R. van Nee, and G. Awater, "Turbo-BLAST and its performance," in *Proc. Vehicular Technology Conf.*, vol. 2, May 2001, pp. 1282–1286.

[18] A. Stefanov and T. Duman, "Turbo-coded modulation for systems with transmit and receive antenna diversity over block fading channels: System model, decoding approaches, and practical considerations," *IEEE J. Select. Areas Commun.*, vol. 19, pp. 958–968, May 2001.

[19] C. Schlegel and A. Grant, "Concatenated space-time coding," in *Proc. Personal, Indoor and Mobile Radio Communications Conf.*, vol. 1, San Diego, CA, Sept. 2001, pp. C139–C143.

[20] S. ten Brink and B. M. Hochwald, "Detection thresholds of iterative MIMO processing," in *Proc. Int. Symp. Information Theory*, July 2002, p. 22.

[21] A. Steiner, M. Peleg, and S. Shamai (Shitz), "Iterative decoding of space–time differentially coded unitary matrix modulation," *IEEE Trans. Signal Processing*, vol. 50, pp. 2385–2395, Oct. 2002.

[22] B. M. Hochwald and S. ten Brink, "Achieving near-capacity on a multiple-antenna channel," *IEEE Trans. Commun.*, vol. 51, pp. 389–399, Mar. 2003.

[23] J. Boutros, N. Gresset, and L. Brunel, "Turbo coding and decoding for multiple antenna channels," in *Proc. 3rd Int. Symp. Turbo Codes, Related Topics*, Brest, France, Sept. 1–5, 2003, pp. 185–186.

[24] S. Haykin and M. Sellathurai, "Turbo-BLAST with multi-loop feedback receiver," in *Proc. 3rd Int. Symp. Turbo Codes, Related Topics*, Brest, France, Sept. 1–5, 2003, pp. 195–202.

[25] K. R. Narayanan and J. Li, "Bandwidth-efficient low-density parity-check coding using multilevel coding and iterative multistage decoding," in *Proc. 2nd Int. Symp. Turbo Codes, Related Topics*, Brest, France, Sept. 4–7, 2000, pp. 165–168.

[26] R. Narayanaswami, "Coded modulation with low-density parity-check codes," Master's thesis, Dept. Elect. Eng., Texas A&M Univ., College Station, TX, 2001.

[27] B. Lu, X. Wang, and K. Narayanan, "LDPC-based space–time coded OFDM systems over correlated fading channels: Performance analysis and receiver design," *IEEE Trans. Commun.*, vol. 50, pp. 74–88, Jan. 2002.

[28] J. Hou, P. H. Siegel, and L. B. Milstein, "Design of LDPC-coded MIMO systems with EXIT chart," in *Proc. 40th Annu. Allerton Conf. Communication, Control, Computers*, Allerton, IL, Oct. 2002, pp. 227–236.

[29] J. Hou, P. H. Siegel, L. B. Milstein, and H. D. Pfister, "Capacity-approaching bandwidth-efficient coded modulation schemes based on low-density parity-check codes," *IEEE Trans. Inform. Theory*, vol. 49, pp. 2141–2155, Sept. 2003.

[30] A. Ashikhmin, G. Kramer, and S. ten Brink, "Extrinsic information transfer functions: A model and two properties," in *Proc. Conf. Information Sciences and Systems*, Princeton, NJ, Mar. 20–22, 2002, pp. 742–747.

[31] S. ten Brink, G. Kramer, and A. Ashikhmin, "Low-density parity-check modulation," in *Proc. Workshop Concepts in Information Theory: A Tribute to Jim Massey*, Breisach, Germany, June 26–28, 2002, pp. 54–57.

[32] M. Tüchler, "Design of serially concatenated systems for long or short block lengths," *IEEE Trans. Commun.*, vol. 52, pp. 209–218, Feb. 2004.

[33] G. Caire, D. Burshtein, and S. Shamai (Shitz), "LDPC coding for interference mitigation at the transmitter," in *Proc. 40th Annu. Allerton Conf. Communication, Control, Computers*, Allerton, IL, Oct. 2002, pp. 217–226.

[34] S. ten Brink and G. Kramer, "Turbo processing for scalar and vector channels," in *Proc. 3rd Int. Symp. Turbo Codes, Related Topics*, Brest, France, Sept. 1–5, 2003, pp. 23–30.

[35] ——, "Design of repeat-accumulate codes for iterative detection and decoding," *IEEE Trans. Signal Processing*, vol. 51, pp. 2764–2772, Nov. 2003.

[36] C. Berrou, A. Glavieux, and P. Thitimajshima, "Near-Shannon limit error-correcting coding and decoding: Turbo codes," in *Proc. Int. Conf. Communications*, vol. 41, May 1993, pp. 1064–1070.

[37] J. Hagenauer, E. Offer, and L. Papke, "Iterative decoding of binary block and convolutional codes," *IEEE Trans. Inform. Theory*, vol. 42, pp. 429–445, Mar. 1996.

[38] E. Sharon, A. Ashikhmin, and S. Litsyn, "EXIT functions for the Gaussian channel," in *Proc. 40th Annu. Allerton Conf. Communication, Control, Computers*, Allerton, IL, Oct. 2003, pp. 972–981.

[39] M. A. Shokrollahi, "New sequences of linear time erasure codes approaching the channel capacity," in *Proc. 13th Conf. Applied Algebra, Error Correcting Codes, and Cryptography*, Berlin, Germany, 1999, pp. 65–76.

[40] M. Tuechler and J. Hagenauer, "EXIT charts and irregular codes," in *Proc. 2002 Conf. Information Sciences and Systems*, Princeton, NJ, Mar. 2002, pp. 748–753.

[41] E. Biglieri, J. Proakis, and S. Shamai (Shitz), "Fading channels: Information theoretic and communications aspects," *IEEE Trans. Inform. Theory*, vol. 44, pp. 2619–2692, Oct. 1998.

[42] I. E. Telatar, "Capacity of multi-antenna Gaussian channels," *Eur. Trans. Telecommun.*, vol. 10, pp. 585–595, Nov. 1999.

[43] G. J. Foschini, "Layered space–time architecture for wireless communication in a fading environment when using multi-element antennas," *Bell Labs. Tech. J.*, vol. 1, no. 2, pp. 41–59, 1996.

[44] "Special issue on MIMO wireless communications," *IEEE Trans. Signal Processing*, vol. 51, pp. 2709–2881, Nov. 2003.

[45] W. H. Press, S. A. Teukolsky, W. T. Vetterling, and B. P. Flannery, *Numerical Recipes in C*. New York: Cambridge Univ. Press, 1997.

[46] E. Sharon, A. Ashikhmin, and S. Litsyn, "EXIT functions for continuous channels—Part I: Constituent codes," *IEEE Trans. Commun.*, submitted for publication.


**Stephan ten Brink** received the Dipl.-Ing. and the Dr.-Ing. degrees in electrical engineering from the University of Stuttgart, Stuttgart, Germany, in 1997 and 2000, respectively.

From 2000 to June 2003, he was with the Wireless Research Laboratory, Bell Laboratories, Lucent Technologies, Holmdel, NJ, conducting research on channel coding for multiple-antenna systems. Since July 2003, he has been with Realtek, Irvine, CA, where he is involved in the development and standardization of high-throughput WLAN systems. His research interests include error-correcting coding, iterative decoding, multiple-antenna communications, and watermarking.

**Gerhard Kramer** (S'91–M'94) received the B.Sc. and M.Sc. degrees in electrical engineering from the University of Manitoba, Winnipeg, MB, Canada, in 1991 and 1992, respectively, and the Dr.Sc. Techn. degree from the Swiss Federal Institute of Technology (ETH), Zürich, Switzerland, in 1998.

From August 1998 to March 2000, he was with Endora Tech AG, Basel, Switzerland, as a communications engineering consultant. Since May 2000, he has been with the Mathematics of Communications Research Department, Bell Laboratories, Lucent Technologies, Murray Hill, NJ.

**Alexei Ashikhmin** (M'00) received the Ph.D. degree in electrical engineering from the Institute for Information Transmission Problems, Russian Academy of Science, Moscow, Russia, in 1994.

From September 1995 to September 1996, he was with the Mathematics Department, Delft University of Technology, Delft, The Netherlands. From January 1997 to July 1999, he was a Postdoctoral Fellow at the Computer, Information, and Communication Division of Los Alamos National Laboratory, Los Alamos, NM. Since 1999, he has been with the Mathematics of Communications Research Department, Bell Laboratories, Lucent Technologies, Murray Hill, NJ. His research interests include information and communication theory, with emphasis on error-correcting codes.

Dr. Ashikhmin currently serves as an Associate Editor for Coding Theory for the IEEE TRANSACTIONS ON INFORMATION THEORY.